A Criterion for the Validity of Parker's Model in Thermal Escape Problems for Planetary Atmospheres

Alexey N. Volkov – University of Alabama

Citation of published version:

Volkov, A. (2015): A Criterion for the Validity of Parker's Model in Thermal Escape Problems for Planetary Atmospheres. *The Astrophysical Journal Letters*, 812(1). DOI: 10.1088/2041-8205/812/1/L1

The Astrophysical Journal Letters, 812:L1 (6pp), 2015 October 10 doi:10.1088/2041-8205/812/1/L1

A CRITERION FOR THE VALIDITY OF PARKER'S MODEL IN THERMAL ESCAPE PROBLEMS FOR PLANETARY ATMOSPHERES

A. N. Volkov
Department of Mechanical Engineering, University of Alabama, Tuscaloosa, AL 35487, USA; avolkov1@ua.edu
Received 2015 May 27; accepted 2015 September 17; published 2015 October 1

ABSTRACT

Mass escape rate of mon- and diatomic gases from a planetary atmosphere is studied based on Parker's model for a broad range of surface conditions. The escape rate is found to follow two asymptotic regimes, namely, high- and low-density regimes, with a short intermediate regime between them. Equations for the escape rate in every asymptotic regime are found theoretically. A comparison of the obtained escape rates with results of recent kinetic simulations shows that Parker's model satisfactorily predicts escape rates only in the high-density regime. Based on this finding, a criterion of applicability of Parker's model for the calculation of the mass escape rate is established.

Key words: Kuiper belt: general – planets and satellites: atmospheres

1. INTRODUCTION

Hydrodynamic modeling based on equations of continuum fluid flows is one of the major approaches for simulation of thermally escaping atmospheric flows. Historically, such models were first applied to study a similar phenomenon of solar wind flow. In particular, Parker (1964a, 1964b) developed a one-dimensional hydrodynamic model of thermal escape from solar corona, assuming that the temperature drops to zero far from the star. Later on, Parker's model became a basis for numerous studies of thermal escape from atmospheres of planetary bodies in the outer solar system (e.g., Watson et al. 1981; Chassefière 1996; Krasnopolsky 1999; Strobel 2008; Zhu et al. 2014) and exoplanets (e.g., Tian et al. 2005; Muñoz 2007).

In order to satisfy the condition of zero temperature far from the surface, it is necessary to continue solution of Parker's model above the exobase into exosphere, where the Fourier law for the heat flux fails (e.g., Volkov et al. 2011a). In spite of this basic flaw, Parker's model has never been systematically tested against kinetic models, which can accurately predict the heat flux and structure of non-equilibriums flow in the exosphere. Thus, the usefulness of Parker's model for thermal escape problems remains questionable.

One-dimensional steady-state hydrodynamic equations of inviscid thermally conducting gas flows have a few distinct types of solutions depending on conditions far from the surface (Freeman & Johnson 1972; Roberts & Soward 1972), including the Chamberlain-type solar breeze solutions with decreasing velocity in the far field (Chamberlain 1961, 1965) and Parker-type solutions with monotonously increasing gas velocity (Parker 1964a, 1964b). The kinetic simulations predict the solar-breeze-type thermally escaping solutions only in conditions of the atmospheric blow-off or transition from the blow-off to Jeans-like escape (Volkov 2014). In the present letter, thermal escape in the Jean-like regime is considered, when the kinetic simulations (Volkov et al. 2013) predict monotonously increasing gas velocity, so that only Parker-type hydrodynamic solutions are chosen for comparison.

The present letter reports for the first time results of systematic comparison of thermal escape rates obtained in hydrodynamic and kinetic simulations. Based on this comparison, the range of surface conditions is found, where Parker's model can be used for calculations of the escape rates. It is shown that Parker's model satisfactorily predicts the escape rate only in the so-called high-density (HD) asymptotic regime. The criterion, determining surface conditions for which Parker's model is capable of quantitative prediction of the escape rate is then established theoretically. Although both hydrodynamic and kinetic simulations are performed for atmospheres without heating, the obtained criterion can be also used to assess the applicability of Parker's model in the externally heated atmospheres based on the parameters on the top of heated atmospheric layer as it is discussed in Section 6.

2. PARKER'S MODEL OF THERMAL ESCAPE

In one-dimensional steady-state atmospheric flows without heating, the distributions of gas density ρ, velocity u, and temperature T can be described by the Navier–Stokes equations

$$r^2\rho u = \Phi_{\rm m}, \tag{1a}$$

$$\rho u u' = -(\rho\Re T)' + \tau'_{rr} + \frac{3\tau_{rr}}{r} - \frac{GM}{r^2}\rho, \tag{1b}$$

$$\Phi_{\rm m}\left(c_pT + \frac{u^2}{2} - \frac{GM}{r}\right) + r^2(q_r - u\tau_{rr}) = \Phi_{\rm e}, \tag{1c}$$

where r is the radial distance, the prime symbol denotes derivatives with respect to r, $\Re = k_{\rm B}/m$, $c_p = (5+\zeta)\Re/2$, $k_{\rm B}$ is the Boltzmann constant, m and ζ are the mass and number of internal degrees of freedom of a molecule, M is planet's mass, G is the gravitational constant, $\Phi_{\rm m}$ and $\Phi_{\rm e}$ are the mass and energy escape rates per steradian, and τ_{rr} and q_r are the viscous stress and heat flux. Atmospheric flows are usually sought with constrains on the surface density ρ_0 and temperature T_0:

$$\text{at} \quad r = r_0: \quad \rho(r_0) = \rho_0, \quad T(r_0) = T_0, \tag{2}$$

where r_0 is the surface radius, and the density is assumed to drop to zero far from the planet:

$$\text{at} \quad r \to \infty: \quad \rho(r) \to 0. \tag{3}$$

Two more boundary conditions are necessary to solve Equations (1), since $\Phi_{\rm m}$ and $\Phi_{\rm e}$ are unknown.

Parker (1964a, 1964b) made three basic assumptions, which helped him to resolve the issue of the missing boundary conditions. First, he considered outflows with a monotonically increasing velocity, which is much smaller than the isothermal sound velocity $\sqrt{\Re T_0}$ at the surface. Second, he assumed that the molecular viscosity plays a marginal role, in which case Equations (1) can be reduced by neglecting τ_{rr}, so that

$$u' = u\,\frac{\frac{2\Re T}{r} - \Re T' - \frac{GM}{r^2}}{u^2 - \Re T}, \tag{4a}$$

$$T' = \frac{\Phi_m\left(c_p T + \frac{u^2}{2} - \frac{GM}{r}\right) - \Phi_e}{r^2\kappa_{00}\left(T/T_{00}\right)^{\omega}}, \tag{4b}$$

where the Fourier law, $q_r = -\kappa dT/dr$, with thermal conductivity, $\kappa = \kappa_{00}(T/T_{00})^{\omega}$ is assumed for the heat flux, and ω is the viscosity exponent. Equations (4) require four boundary conditions, so that Parker (1964a, 1964b) finally assumed that the temperature should drop to zero far from the surface:

$$\text{at} \qquad r \to \infty: \quad T(r) \to 0. \tag{5}$$

In this model, the isothermal Mach number $Ma = u/\sqrt{\Re T}$ evolves from $Ma_0 = u_0/\sqrt{\Re T_0} \ll 1$ at $r = r_0$ to infinity at $r \to \infty$, i.e., the flow passes through the isothermal sonic point, where $u = \sqrt{\Re T}$ and the denominator of Equation (4a) is equal to zero. Distributions of gas parameters are continuous only if the numerator becomes zero simultaneously with the denominator, i.e., the isothermal sonic point is the critical point of Equations (4). Using Equation (4b) in order to exclude T' from the consideration at the critical point, one can obtain

$$\Phi_e = \Phi_m\left(c_p T_c + \frac{u_c^2}{2} - \frac{GM}{r_c}\right) + \frac{GM\kappa_c}{\Re} - 2T_c r_c \kappa_c, \tag{6}$$

where subscript "c" denotes parameters in the critical point. This equation shows that gas parameters at the critical point and escape rates are not independent of each other. For a solution passing through the critical point with monotonically increasing velocity, the density drops as $1/r^2$ far from the surface and Equation (3) is satisfied automatically, so it should be excluded from consideration and replaced by Equation (6).

Thus, Parker's model implies a solution of Equation (4) with boundary conditions given by Equations (2) and (5) starting at the surface with $Ma_0 < 1$ and passing through a critical point, where atmospheric parameters satisfy Equation (6).

3. NUMERICAL APPROACH FOR SOLVING EQUATIONS OF PARKER'S MODEL

In the present paper, Parker's model is analyzed in a dimensionless form in order to reduce the number of parameters governing the solutions. Equation (4) is re-written in terms of dimensionless variables $\bar r = r/r_c$, $\bar T = T/T_c$, and $\bar u = u/\sqrt{\Re T_c}$ as

$$\bar u' = \bar u\,\frac{\frac{2\bar T}{\bar r} - \bar T' - \frac{\lambda_c}{\bar r^2}}{\bar u^2 - \bar T}, \tag{7a}$$

$$\bar T' = \frac{\varphi_m}{\bar r^2 \bar T^{\omega}}\left(\frac{\gamma}{\gamma - 1}\bar T + \frac{\bar u^2}{2} - \frac{\lambda_c}{\bar r} - \Psi_e\right), \tag{7b}$$

where the prime symbol denotes derivatives with respect to $\bar r$, $\gamma = (\zeta + 5)/(\zeta + 3)$, $\lambda_c = GM/(\Re T_c r_c)$ is the Jeans parameter at the critical point, $\varphi_m = \Re\Phi_m/(\kappa_c r_c)$, and $\Psi_e = \Phi_e/(\Re T_c \Phi_m)$. Equation (6) in reduced units transforms into

$$\Psi_e = \frac{\gamma}{\gamma - 1} + \frac{1}{2} + \frac{\lambda_c - 2}{\varphi_m} - \lambda_c. \tag{8}$$

Solution of Parker's model in reduced units depends only on two surface parameters, e.g., Jeans parameter $\lambda_0 = GM/(\Re T_0 r_0) = \lambda_c/(\bar r_0 \bar T_0)$ and Knudsen number $Kn_0 = l_{mfp,0}/L_0$, characterizing the strength of the gravitational field and degree of atmosphere rarefaction at the surface. Assuming that the mean free path of gas molecules $l_{mfp,0}$ is given by the first approximation of the Chapmen-Enskog theory for the Variable Hard Sphere (VHS) molecular model (Bird 1994), and the atmospheric length scale L_0 is equal to r_0, one can find that $Kn_0 = K\kappa(T_0)/\left(\sqrt{\Re T_0}\rho_0 r_0 \Re\right) = Kn_c \bar T_0^{\omega - 1/2}\bar r_0 \bar u_0$, where Kn_c is the Knudsen number at the critical point

$$Kn_c = \frac{K}{\varphi_m}, \qquad K = \frac{2(5 - 2\omega)(7 - 2\omega)}{15\sqrt{2\pi}}\frac{\gamma - 1}{\gamma}\mathrm{Pr} \tag{9}$$

and Pr is the Prandtl number.

A solution of Equation (7) for the surface conditions given by λ_0 and Kn_0 can be obtained using a two-step approach. At the first downstream step, Equation (7) is solved in the downstream direction from the critical point, $\bar r > 1$, for a fixed λ_c with the initial conditions

$$\bar u(1) = 1, \qquad \bar T(1) = 1 \tag{10}$$

and Ψ_e given by Equation (8). These equations are solved iteratively by varying φ_m, until a φ_m is found that the condition

$$\text{at } \bar r \to \infty: \quad \bar T \to 0 \tag{11}$$

is satisfied. By repeating this iterative procedure for various λ_c, the dependence $\varphi_m = \varphi_m(\lambda_c)$ can be obtained numerically. At the second upstream step, Equation (7) are solved with the initial conditions given by Equation (10) in the upstream direction, $\bar r < 1$, for fixed λ_0 and Kn_0. For $Kn_0 < Kn_c$, one can iteratively find such λ_c and $\bar r_0$ that Jeans parameter and Knudsen number at $\bar r = \bar r_0$ are equal to λ_0 and Kn_0. Once the dependences $\lambda_c(\lambda_0, Kn_0)$ and $\bar r_0(\lambda_0, Kn_0)$ are established, they can be used in order to find any solution of Parker's model for a given surface condition. Typical dependences of λ_c on λ_0 and Kn_0 are shown in Figure 1. It is remarkable that λ_c varies within a narrow range at small Kn_0 and large λ_0 for arbitrary γ and ω.

4. ESCAPE RATES IN PARKER'S AND KINETIC MODELS

Numerical calculations with Parker's model were performed for mon- ($\zeta = 0$, $\gamma = 5/3$) and diatomic ($\zeta = 2$, $\gamma = 7/5$) gases with Pr = 2/3 and for $\omega = 3/4$, and $\omega = 1$. The mass escape rate is calculated in reduced units as

$$\frac{\Phi_m}{\Phi_{m(J0)}} = \sqrt{2\pi}\,Ma_0\frac{\exp(\lambda_0)}{\lambda_0 + 1}, \tag{12}$$

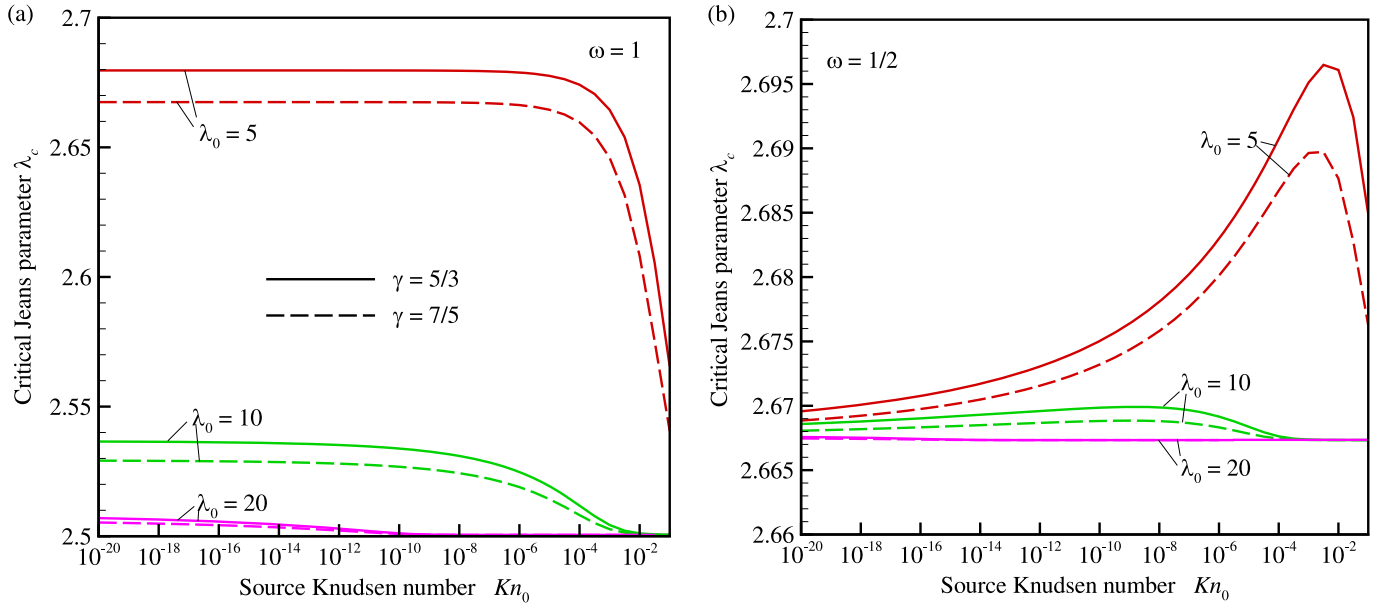

Figure 1. Jeans parameter at the critical point λ_c vs. surface Knudsen number Kn_0 obtained with Parker's model at $\gamma = 5/3$ (solid curves) and $\gamma = 7/5$ (dashed curves) for $\omega = 1$ (a) and $\omega = 1/2$ (b) and various surface Jeans parameters: $\lambda_0 = 5$, $\lambda_0 = 10$, and $\lambda_0 = 20$.

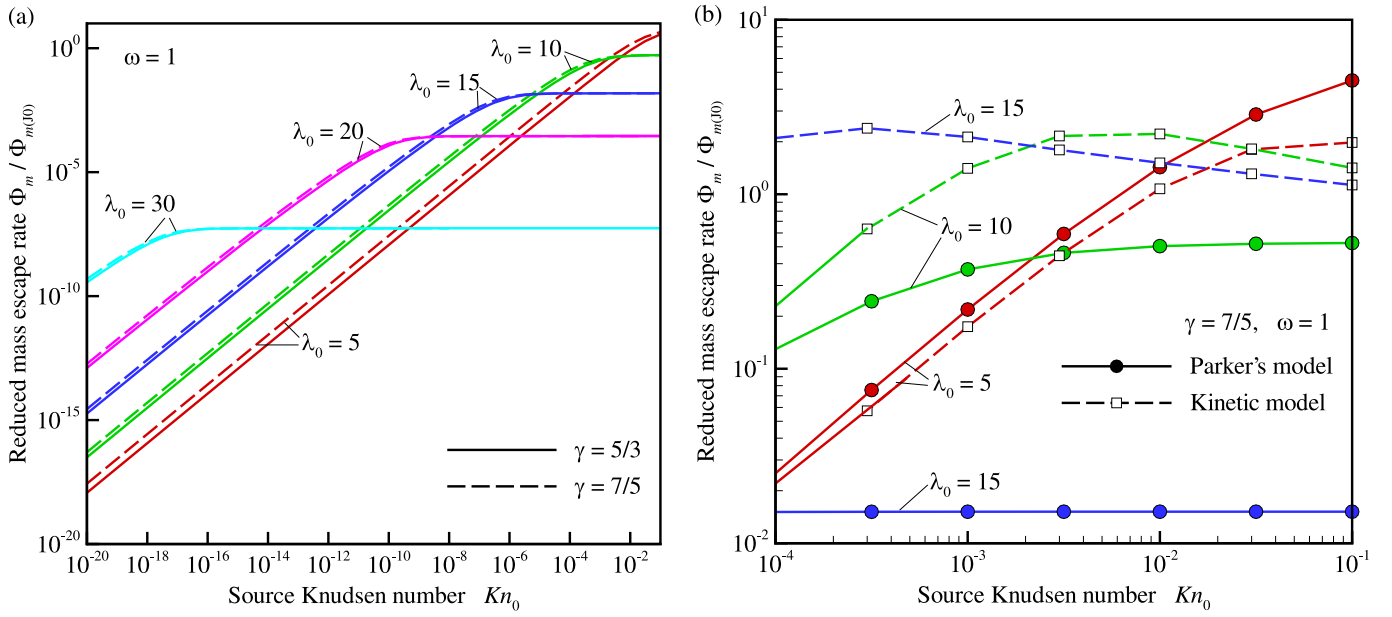

Figure 2. Reduced mass escape rate $\Phi_m/\Phi_{m(J0)}$ vs. surface Knudsen number Kn_0 for various λ_0. In panel (a), all curves are obtained with Parker's model for $\gamma = 5/3$ (solid curves) $\gamma = 7/5$ (dashed curves) at $\omega = 1$. In panel (b), curves are obtained for $\gamma = 7/5$ and $\omega = 1$ with the kinetic (Volkov et al. 2011a, 2013; dashed curves) and Parker's (solid curves) models.

where Ma_0 and $\Phi_{m(J0)}$ are the Mach number and Jeans escape rate at the surface:

$$Ma_0 = \frac{Kn_0}{Kn_c}\frac{\lambda_0}{\lambda_c}\bar{T}_0^{1-\omega}, \tag{13}$$

$$\Phi_{m(J0)} = r_0^2\rho_0\sqrt{\frac{\Re T_0}{2\pi}}\left(\lambda_0+1\right)\exp\left(-\lambda_0\right). \tag{14}$$

The dependences of $\Phi_m/\Phi_{m(J0)}$ on Kn_0 at fixed λ_0 are found to be qualitatively similar for all γ and ω considered and include two asymptotic regimes, which correspond to the case of large and small Kn_0, and intermediate regime, corresponding to transition between these asymptotic regimes (Figure 2(a)). Following Parker (1964b), the case, when $\Phi_m/\Phi_{m(J0)}$ asymptotically does not depend on Kn_0, can be called the low-density (LD) regime and the case, when $\Phi_m/\Phi_{m(J0)}$ asymptotically varies as $1/Kn_0$, can be called the HD regime.

The escape rates calculated with Parker's model are found to be in quantitative agreement with results of recent kinetic simulations performed by Volkov et al. (2011a, 2013) only in the HD regime (Figure 2(b)), when values of $\Phi_m/\Phi_{m(J0)}$ calculated with both models asymptotically approach each other with decreasing Kn_0 as it is seen for $\lambda_0 = 5$ and $\lambda_0 = 10$. At $\lambda_0 = 15$, the escape rates disagree in the considered range of Kn_0, but they presumably agree at smaller Kn_0, where the results of kinetic simulations are not currently available. In the

LD regime, kinetic Φ_m approaches $\Phi_{m(J0)}$ at $Kn_0 \to \infty$, when the effects of intermolecular collisions become progressively less important and escaping flows evolve in the free molecular flow regime. On the contrary, $\Phi_m/\Phi_{m(J0)}$ predicted by Parker's model at $Kn_0 \to \infty$ can be both larger and many orders of magnitude smaller than 1. For instance, in the range $\lambda_0 = 15$–20, which is characteristic for a number of large Kuiper Belt objects (KBOs, Johnson et al. 2015), the maximum values of $\Phi_m/\Phi_{m(J0)}$ are in the order of 10^{-2}–10^{-4}.

5. CRITERION OF VALIDITY OF PARKER'S MODEL

The goal of the present section is to formulate a criterion of validity of Parker's model in terms of λ_0 and Kn_0 for arbitrary γ and ω. For this purpose, accurate expressions for $\Phi_m/\Phi_{m(J0)}$ in both HD and LD regimes are obtained first.

In the LD regime, the Knudsen number is large everywhere, including at the critical point, and φ_m is small according to Equation (9). Following Parker (1964b), one can consider the only case when $\Phi_e = \varphi_m \Psi_e T_c \kappa_c r_c > 0$ and integrate Equation (7b) neglecting all terms in the right-hand side of this equation with exception of Ψ_e. Solution of the obtained equation satisfies Equation (11) if $\lambda_c = \lambda_{c(min)} = (2\omega + 3)/(\omega + 1)$, $\varphi_m \Psi_e = 1/(\omega + 1)$, and temperature varies as (Parker 1964b)

$$\bar{T} = \bar{r}^{-\frac{1}{\omega+1}}. \tag{15}$$

The critical Jeans parameter in the LD regime $\lambda_{c(min)}$ corresponds to the minimum possible λ_c for a gas with given ω. If $\bar{r} \ll 1$, then the term with $\bar{u}^2$ in the right-hand side of Equation (7a) can be neglected and gas velocity far upstream of the critical point varies as (A. N. Volkov 2015, in preparation)

$$\bar{u} = V_0(\omega)\bar{r}^{-\frac{2\omega+3}{\omega+1}} \exp\left[\frac{2\omega+3}{\omega}\left(1 - \bar{r}^{-\frac{\omega}{\omega+1}}\right)\right], \tag{16}$$

where the coefficient $V_0(\omega)$ is given by the condition that Equation (16) matches the accurate solution of Equation (7a) at $\bar{r} \ll 1$. The analysis of numerical solutions of Parkers model showed that $V_0(\omega)$ varies from ~0.708 to ~0.6725 when ω increases from 1/2 to 1 and can be fitted to the power law $V_0(\omega) = 0.672/\omega^{0.0742}$. Since $\bar{r}_0 = \left(\lambda_{c(min)}/\lambda_0\right)^{(\omega+1)/\omega}$, Equations (15) and (16) allow one to calculate the surface Mach number $Ma_{0(L)}$ and escape rate $\Phi_{m(L)}$ in the LD regime as

$$Ma_{0(L)} = V_0(\omega)\left(\frac{\omega+1}{2\omega+3}\lambda_0\right)^{\frac{2\omega+5/2}{\omega}} \times \exp\left(\frac{2\omega+3}{\omega} - \frac{\omega+1}{\omega}\lambda_0\right), \tag{17}$$

$$\frac{\Phi_{m(L)}}{\Phi_{m(J0)}} = \frac{\sqrt{2\pi}}{\lambda_0+1} V_0(\omega)\left(\frac{\omega+1}{2\omega+3}\lambda_0\right)^{\frac{2\omega+5/2}{\omega}} \times \exp\left(\frac{2\omega+3}{\omega} - \frac{\lambda_0}{\omega}\right). \tag{18}$$

In order to find an equation for the escape rate in the HD regime the definition of λ_0 can be re-written to represent the surface temperature as a function of λ_0 and Kn_0:

$$\bar{T}_0 = \frac{\lambda_c(\lambda_0, Kn_0)/\lambda_0}{\bar{r}_0(\lambda_0, Kn_0)}. \tag{19}$$

With exception of the case, when λ_0 is close to $\gamma/(\gamma - 1)$, solutions of Parker's model at various λ_0 correspond to $\lambda_c \approx \lambda_{c(min)}$ (Figure 1). Such "upstream" solutions start at large Knudsen numbers at the critical point and then, with decreasing $\bar{r}$, first follow Parker's LD approximation. Then they gradually approach another limit solution corresponding to the case of small surface Knudsen number, i.e., Parker's HD approximation. Then surface temperature and its gradient can be found as

$$\bar{T}_0 = \frac{\lambda_{c(min)}/\lambda_0}{\bar{r}_0(\lambda_0, Kn_0)}, \tag{20}$$

$$\left.\frac{d\bar{T}}{d\bar{r}}\right|_{\bar{r}=\bar{r}_0} \approx -\frac{\lambda_{c(min)}/\lambda_0}{\bar{r}_0^2}. \tag{21}$$

Equation (7b) can be re-written at $\bar{r} = \bar{r}_0$ as

$$\bar{r}_0^2 \bar{T}_0^{\omega-1}\left.\frac{d\bar{T}}{d\bar{r}}\right|_{\bar{r}=\bar{r}_0} = \varphi_m\left(\frac{\gamma}{\gamma-1} + \frac{Ma_0^2}{2} - \lambda_0 - \frac{\Psi_e}{\bar{T}_0}\right). \tag{22}$$

By excluding the derivative from Equations (21) and (22) in the HD regime, when $Ma_0 \ll 1$ and $\bar{T}_0 \gg 1$, one can obtain

$$\varphi_m \bar{T}_0^{1-\omega} = \frac{\lambda_{c(min)}/\lambda_0}{\lambda_0 - \frac{\gamma}{\gamma-1}}. \tag{23}$$

This equation can be used in order to calculate the surface Mach number and escape rate in the HD regime based on Equation (12) as

$$Ma_{0(H)} = \frac{Kn_0}{K}\frac{\lambda_0}{\lambda_{c(min)}}\varphi_m \bar{T}_0^{1-\omega} = \frac{Kn_0}{K\left(\lambda_0 - \frac{\gamma}{\gamma-1}\right)}, \tag{24}$$

$$\frac{\Phi_{m(H)}}{\Phi_{m(J0)}} = \sqrt{2\pi} Ma_{0(H)} \frac{\exp(\lambda_0)}{\lambda_0+1}. \tag{25}$$

The numerical values of the escape rate closely approach the solutions given by Equations (18) and (25) as shown in Figure 3 for $\gamma = 7/5$ and $\omega = 1$. Calculations for $\gamma = 5/3$ and/or various ω from 1/2 to 1 demonstrate similar degree of agreement between obtained equations and numerical $\Phi_m/\Phi_{m(J0)}$. Both equations, however, become inaccurate when λ_0 closely approaches $\gamma/(\gamma - 1)$.

As it was shown in Section 4, Parker's model enables quantitative prediction of Φ_m only in the HD regime. Based on Equations (17) and (24), this criterion of validity of Parker's model can be now formulated as

$$Ma_{0(H)} \ll Ma_{0(L)}. \tag{26}$$

or

$$Kn_0 \ll Kn_P, \tag{27}$$

where the "turning" Knudsen number Kn_P

$$Kn_p = K\, V_0(\omega)\left(\frac{\omega+1}{2\omega+3}\lambda_0\right)^{\frac{2\omega+5/2}{\omega}} \times \exp\left(\frac{2\omega+3}{\omega} - \frac{\omega+1}{\omega}\lambda_0\right)\left(\lambda_0 - \frac{\gamma}{\gamma-1}\right) \tag{28}$$

corresponds to the nominal point where the dependence of the escape rate Kn_0 turns from the LD to HD regime. A comparison

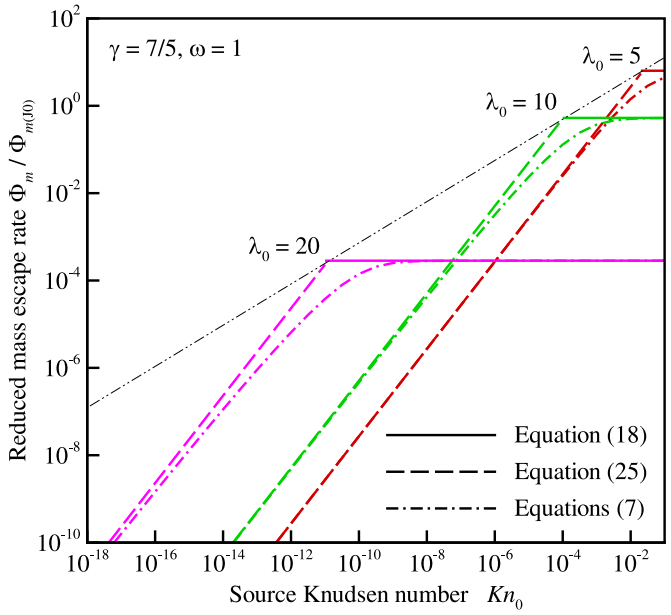

Figure 3. Reduced mass escape rate $\Phi_m/\Phi_{m(J0)}$ vs. Knudsen number Kn_0 obtained as a result of direct numerical solution of Equation (7) (dashed–dotted curves), with Equation (18) for the HD regime (dashed lines), and with Equation (18) for the LD regime (solid curves) at $\gamma = 7/5$, $\omega = 1$, and $\lambda_0 = 5$, $\lambda_0 = 10$, and $\lambda_0 = 20$. Dashed-double-dotted line corresponds to points where $Ma_{0(H)} = Ma_{0(L)}$ or $Kn_0 = Kn_P$.

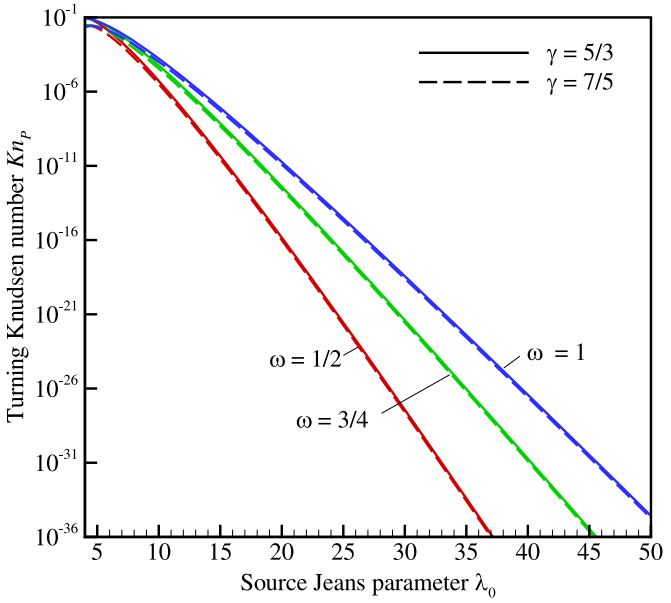

Figure 4. Turning Knudsen number Kn_P given by Equation (28) vs. surface Jeans parameter λ_0 for $\gamma = 5/3$ (solid curves) and $\gamma = 7/5$ (dashed curves) at $\omega = 1/2$, $\omega = 3/4$, and $\omega = 1$.

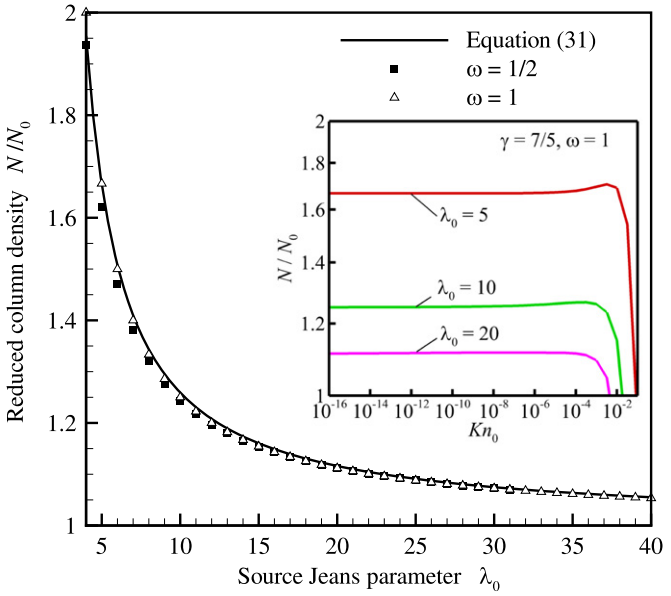

Figure 5. Reduced column density N/N_0 vs. Jeans parameter λ_0 obtained with Parker's model in the limit $Kn_0 \to 0$ at $\omega = 1/2$ (square symbols) and $\omega = 1$ (triangle symbols). Solid curve corresponds to Equation (31). Calculated values of N/N_0 for $\gamma = 5/3$ and $\gamma = 7/5$ visually coincide with each other at $Kn_0 \to 0$. The inset shows N/N_0 vs. Kn_0 obtained at $\gamma = 5/3$ and $\omega = 1$ for $\lambda_0 = 5$, $\lambda_0 = 10$, and $\lambda_0 = 20$.

of Parker's solutions with results of kinetic simulations at $\lambda_0 = 5$ and $\lambda_0 = 10$ shows that Parker's escape rate is within a factor of two from the kinetic rate if $Kn_0/Kn_P < 10^{-2} - 10^{-1}$. The turning Knudsen number, Kn_P, is a strong function of ω, but only marginally depends on γ (Figure 4). At fixed λ_0, Parker's model is valid in a substantially broader range of Kn_0 in the pseudo-Maxwellian gas ($\omega = 1$) than in the hard sphere gas ($\omega = 1/2$).

The criterion of validity of Parker's model can be also formulated in terms of integral atmospheric parameters, which can be directly deduced from the analysis of absorption spectra of planetary bodies or probing the atmospheres during stellar occultation, e.g., the column density N

$$N = \int_{r_0}^{r_x} \frac{\rho}{m} dr. \tag{29}$$

Here r_x is the radial position of the nominal exobase, where the mean free path of gas molecules $l_{mfp}(r_x)$ is equal to the atmospheric scale height $H(r_x) = r_x/\lambda_x$ ($\lambda_x = GM/(\Re T_x r_x)$ is the exobase Jeans parameter). Assuming the barometric distribution of molecules with the scale height $H_0 = r_0/\lambda_0$, $\rho = \rho_0 \exp((r_0 - r)/H_0)$, the first approximation to the column density at large λ_0 is

$$N \sim N_0 = \frac{\rho_0 H_0}{m} = \frac{1}{\Sigma_T(T_0)} \frac{1}{\lambda_0 Kn_0}, \tag{30}$$

where for the VHS model of intermolecular collisions $\Sigma_T(T_0) = k_B\sqrt{\Re T_0}/[K\kappa(T_0)] = \sqrt{2}\,\sigma_T(T_0)$ and $\sigma_T(T_0)$ is the total collision cross section of molecules at temperature T_0 (Johnson et al. 2015) with typical value in the order of 10^{-14} cm^{-2} for atmospheric species like N_2 or CH_4 (Bird 1994). The examples of dependences of N/N_0 on Kn_0 at various λ_0 obtained for a monatomic gas with $\omega = 1$ are shown in the inset of Figure 5. It is seen that N/N_0 is independent of Kn_0 if $Kn_0 < 10^{-5}$. Calculated values of N/N_0 in the limit of small Kn_0 are shown in Figure 5 by symbols. These values marginally depend on γ and ω, so that the ratio N/N_0 can be considered as a function of only λ_0 and fitted at $\lambda_0 \geqslant 4$ by equation

$$\frac{N}{N_0} = \frac{1 + \lambda_0 + \exp(4/\lambda_0)}{\lambda_0}, \tag{31}$$

shown in Figure 5 by the solid curve. Then the criterion given by Equations (27) and (28) can be reformulated in terms of N as

$$N \gg N_P = \frac{1}{\sqrt{2}\,\sigma_T(T_0)} \frac{1 + \lambda_0 + \exp\left(\frac{4}{\lambda_0}\right)}{\lambda_0^2} \frac{1}{Kn_P}. \quad (32)$$

6. DISCUSSION AND CONCLUSION

The developed criterion for the validity of Parker's model for thermal escape problems can be directly applied for atmospheres without substantial external heating. Certain KBOs, including dwarf planets in the outer solar system, may have such atmospheres. The degree of absorption of solar radiation in KBO atmospheres depends on atmospheric column (Johnson et al. 2015) and, in particular, on the abundance of methane, which is the primary absorbing agent in presumably nitrogen-rich KBO atmospheres (Strobel et al. 1996; Krasnopolsky & Cruikshank 1999). Currently the abundance of methane is not well-constrained for the majority of KBOs with exception of Pluto and Charon (see review of literature data, e.g., in Johnson et al. 2015). For Sedna and Quaoar, which have relatively thin and thick atmospheres ($N \approx 10^{17}$ cm^{-2} and $N \approx 10^{21}$ cm^{-2}) at $\lambda \approx 15$ in solar-maximum conditions (Johnson et al. 2015), $Kn_0 \approx 7 \cdot 10^{-5}$ and $Kn_0 \approx 7 \cdot 10^{-9}$, while $Kn_p \approx 5 \cdot 10^{-8}$. For KBOs like Pluto with larger λ_0, the condition given by Equation (28) is even more restrictive. Thus, Parker's model is not applicable for the majority of KBOs, which atmospheres do not contain sufficient amount of CH_4 to be heated by solar radiation.

For planetary atmospheres with external heating, the criterion given by Equation (28) can be used with certain approximations, assuming that λ_0 and Kn_0 characterize flow conditions at the top of the heated layer. These conditions are more favorable for application of Parker's model above the heated layer because of increase in the local Jeans parameter. With increasing amount of absorbed energy and decreasing Jeans parameter at the upper boundary of the heated layer, the critical point approaches the exobase, and Parker's and kinetic model can produce similar escape rates as it is apparent from the comparison of curves for $\lambda_0 = 5$ in Figure 2(b). This is in agreement with findings by Zhu et al. (2014), who concluded that Pluto's exobase is locked at $\lambda_x = 4$–6, and Parker's model escape rate is different from the enhanced Jeans rate predicted in kinetic simulations by Volkov et al. (2011a, 2011b) by the factor of 1–0.22. For less intensive heating, which can be specific to other dwarf planets, Parker's model applied to the part of the atmosphere above the heated layer can substantially underestimate the escape rate.

In conclusion, the numerical study of Parker's model reveals that two asymptotic regimes can occur depending on the surface conditions. The escape rates in these regimes are calculated theoretically in the form of Equations (18) and (25). Escape rates predicted by Parker's and kinetic models agree only in the HD asymptotic regime. The criterion of applicability of Parker's model is then given by Equations (27) and (28) or (32).

This research was supported by the NASA Planetary Atmospheres Program. The author thanks Prof. R. E. Johnson for helpful comments on the results discussed in the present paper.

REFERENCES

Bird, G. A. 1994, Molecular Gas Dynamics and the Direct Simulation of Gas Flows (Oxford: Clarendon)
Chamberlain, J. W. 1961, ApJ, 133, 675
Chamberlain, J. W. 1965, ApJ, 141, 320
Chassefière, E. 1996, JGR, 101, 26039
Freeman, N. C., & Johnson, R. S. 1972, RSPSA, 329, 241
Johnson, R. E., Oza, A., Young, L. A., Volkov, A. N., & Schmidt, C. 2015, ApJ, 809, 43
Krasnopolsky, V. A. 1999, JGR, 104, 5955
Krasnopolsky, V. A., & Cruikshank, D. P. 1999, JGR, 104, 21979
Muñoz, A. G. 2007, P&SS, 55, 1426
Parker, E. N. 1964a, ApJ, 139, 72
Parker, E. N. 1964b, ApJ, 139, 93
Roberts, P. H., & Soward, A. M. 1972, RSPSA, 328, 185
Strobel, D. F. 2008, Icar, 193, 612
Strobel, D. F., Zhu, X., Summers, M. E., & Stevens, M. H. 1996, Icar, 120, 266
Tian, F., Toon, O. B., Pavlov, A. A., & De Sterck, H. 2005, ApJ, 621, 1049
Volkov, A. N. 2014, Vacuu, 109, 308
Volkov, A. N., Johnson, R. E., & Tucker, O. J. 2013, FlDy, 48, 239
Volkov, A. N., Johnson, R. E., Tucker, O. J., & Erwin, J. T. 2011a, ApJL, 729, L24
Volkov, A. N., Tucker, O. J., Erwin, J. T., & Johnson, R. E. 2011b, PhFl, 23, 066601
Watson, A. J., Donahue, T. M., & Walker, J. C. 1981, Icar, 48, 150
Zhu, X., Strobel, D. F., & Erwin, J. T. 2014, Icar, 228, 301